Towards Automated Materials Analysis: Deep Learning Denoising and Phase Identification from 4D-STEM

Pok Man Ethan Lo[1] and Fanzhi Su[1]

[1]Department of Materials Science and Metallurgy, University of Cambridge, UK

1 Objective

Ni-rich layered cathodes such as $LiNi_{0.8}Mn_{0.1}Co_{0.1}O_2$ (NMC811) are promising as the next generation battery, but their degradation mechanisms remain poorly understood due to nanoscale structural deviations. 4D scanning transmission electron microscopy (4D-STEM) reveals nanoscale information: the inspection of local phases and crystal structure through diffraction patterns (DPs). Yet, these DPs suffer from low signal-to-noise ratio contributed by complex background noise and weak reflections. Here, we present an automated phase searching algorithm supported by deep-learning based denoising strategies enabling the reliable identification of the O1 and O3 phase, key to analysing the performance of the Ni-rich layered cathodes.

2 Methodology

Clean diffraction patterns (DPs) were simulated using data obtained from Materials Project [1]. Using 435 materials simulated over 60 zone axis, yielding over 28,000 diffraction patterns. Each DP was subjected to a composite noise model to simulate the experimental 4D-STEM conditions, which includes: (i) Poisson noise, (ii) halo background centred about the transmitted beam, (iii) Gaussian blurring to mimic finite detector point-spread and inelastic contributions, and (iv) salt and pepper noise. Spot-dimming and/or beam-stop-like attenuation were also added to simulate common artefacts in 4D-STEM. This produced clean-noisy pair DPs for training (exemplified in Figure 1). A dense U-Net structure was favoured over the typical U-Net structure to train the denoising procedure as it allows deeper global features to be extracted [2]. The trained model was then evaluated using experimentally collected 4D-STEM images of NMC811. Phase identification was then performed using the workflow on the denoised DPs. O1/O3 phases in DPs were found by first identifying diffraction spots within a defined annular region where the O1 and O3 phase reflections are expected. A Difference-of-Gaussians (DoG) approach was then used to detect local intensity peaks. Phase detection was carried out using a RANSAC (random sample consensus) procedure: two reflection spots were randomly sampled to generate a regular hexagon template, and the predicted vertices were matched to nearby detected spots. Only templates with sufficient vertex matches within a distance tolerance were retained. The identified hexagons were then separated into phases based on their normalised radius (i.e., distance from the [000] central beam) relative to the learned O1 and O3 ring radii.

3 Results, Conclusions, and Future Works

As demonstrated in Figure 2, the workflow can be applied to experimental DPs with extremely low signal-to-noise ratio and identify the reflections corresponding to O3 and O1 accurately. Here, only the central annular region of the DP was kept to minimise the analysis needed on each DP as the O1 and O3 phase was centred near the [000] peak. The identification result is then summarised by a data grid for material phase distribution analysis. As shown in Figure 3a, DPs were extracted from the green rectangular region of interest (ROI) in the HAADF image of a NMC811 cathode material and analysed to generate a heatmap showing the phase distribution (Figure 3b). In the phase distribution map, the pixels where extracted DPs contain O3 or O1 phase were highlighted in orange and blue, respectively. The pixels coloured grey are regions of both O3 and O1 phase present. Here, work has been done to develop a phase identification workflow suited for the identification of the O1 and O3 phase. This work is a proof of concept for the ability to denoise and phase identify experimental 4D STEM images, the workflow can be extended beyond the cathode material, supporting different materials and conditions with minimal manual intervention.

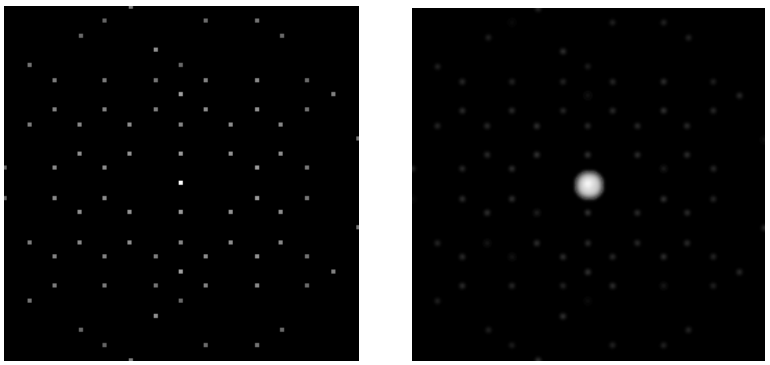

(a) (b)

Figure 1: Example of paired dataset ((a) clean version, (b) noisy version) used for RDUnet training.

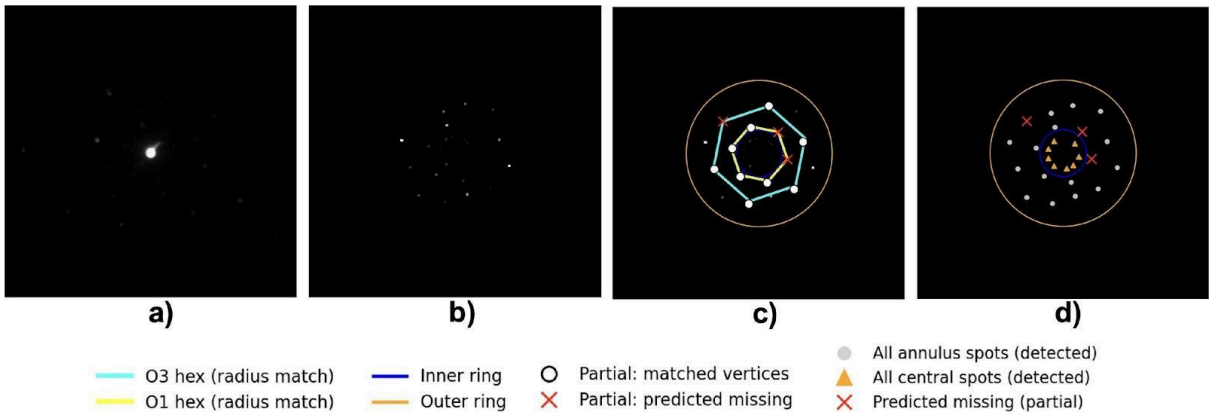

Figure 2: (a) Original image. (b) Denoised image. (c) Hexagon detection overlay on the denoised image:cyan (O3 phase) and yellow (O1 phase). (d) Detected spots on a black canvas, with crosses indicating the predicted spots and the orange triangle showing spots found outside the annular region.

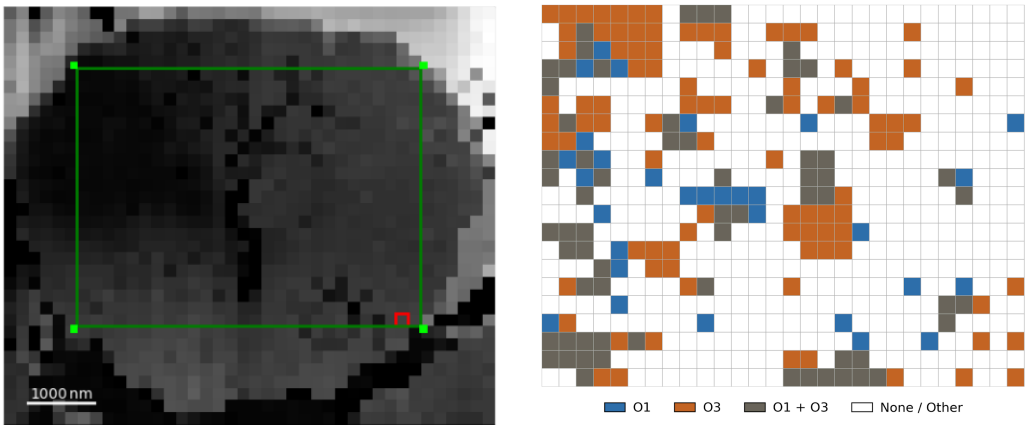

(a) (b)

Figure 3: (a) The ROI (highlighted by the green oval) in an NMC811 HAADF image, where the DPs were extracted. b) Phase distribution map within the ROI. Each pixel corresponds to a probe position and is labelled using O1/O3 diagnostic reflections from the denoised DP.

References

[1] Shyue Ping Ong, Shreyas Cholia, Anubhav Jain, Miriam Brafman, Dan Gunter, Gerbrand Ceder, and Kristin A. Persson. The materials application programming interface (API): A simple, flexible and efficient API for materials data based on REpresentational state transfer (REST) principles. *Computational Materials Science*, 97:209–215, feb 2015. doi: 10.1016/j.commatsci.2014.10.037. URL `http://dx.doi.org/10.1016/j.commatsci.2014.10.037`.

[2] Javier Gurrola-Ramos, Oscar Dalmau, and Teresa E Alarco´n. A residual dense u-net neural network for image denoising. *IEEE Access*, 9:31742–31754, 2021. doi: 10.1109/ACCESS.2021.3061062.